

Proceedings of the Institution of Mechanical Engineers, Part J: Journal of Engineering Tribology

<http://pij.sagepub.com/>

Effects of bearing clearance and supporting stiffness on performances of rotor-bearing system with multi-decked protuberant gas foil journal bearing

Tianwei Lai, Shuangtao Chen, Bin Ma, Yueqing Zheng and Yu Hou

Proceedings of the Institution of Mechanical Engineers, Part J: Journal of Engineering Tribology published online 25 April 2014

DOI: 10.1177/1350650114531406

The online version of this article can be found at:

<http://pij.sagepub.com/content/early/2014/04/24/1350650114531406>

Published by:



<http://www.sagepublications.com>

On behalf of:



Institution of Mechanical Engineers

Additional services and information for *Proceedings of the Institution of Mechanical Engineers, Part J: Journal of Engineering Tribology* can be found at:

Email Alerts: <http://pij.sagepub.com/cgi/alerts>

Subscriptions: <http://pij.sagepub.com/subscriptions>

Reprints: <http://www.sagepub.com/journalsReprints.nav>

Permissions: <http://www.sagepub.com/journalsPermissions.nav>

Citations: <http://pij.sagepub.com/content/early/2014/04/24/1350650114531406.refs.html>

>> [OnlineFirst Version of Record](#) - Apr 25, 2014

[What is This?](#)

Effects of bearing clearance and supporting stiffness on performances of rotor-bearing system with multi-decked protuberant gas foil journal bearing

Proc IMechE Part J:
J Engineering Tribology
0(0) 1–9
© IMechE 2014
Reprints and permissions:
sagepub.co.uk/journalsPermissions.nav
DOI: 10.1177/1350650114531406
pij.sagepub.com


Tianwei Lai¹, Shuangtao Chen¹, Bin Ma¹, Yueqing Zheng^{1,2} and Yu Hou^{1,3}

Abstract

The supporting stiffness and coulomb damping in a bearing play significant roles in the smooth operation of rotor-bearing system. The performance of multi-decked protuberant gas foil journal bearing is evaluated experimentally in a high-speed turboexpander. The effect of radial clearance on the bearing performance is analyzed based on the relationship between rotor speed and supply pressure in the speed-up and speed-down processes. The maximal speed of the 25 mm diameter rotor reached as high as 100 kr/min, and subsynchronous vibrations are suppressed in the tests. For the bearings with 0.05 mm protuberant foils, there will be thermal runaway problem with $-20\ \mu\text{m}$ clearance, while unstable operation appears with $80\ \mu\text{m}$ clearance. For the bearing with 0.07 mm protuberant foil, the vibration amplitude is constrained within smaller amplitude due to stiffer supporting structure. The test results indicate that the bearing can operate stably under different gas film thickness and supporting stiffness, and that this kind of foil bearing can be applied in high-speed turbomachinery due to its stability and adaptability.

Keywords

Turboexpander, multi-decked, foil bearing, bearing clearance, supporting stiffness

Date received: 23 December 2013; accepted: 21 March 2014

Introduction

Compliant surface foil bearing outperforms other bearings for high-speed applications since proposed by Blok and Rossum¹ in the 1950s. It has been widely used in high-speed rotational machineries including turborefrigerator, gas turbine, turboexpander, and centrifugal compressor.^{2–5} Foil bearing is also a promising candidate for applications under extreme working temperatures.^{4,6–8} Compliant surface bearings are generally used with a moderate preload on the journal. The stability advantage can be attributed to the compliant property of foils, which depends on the structural and hydrodynamic stiffness.^{9,10} Therefore, it is crucial to choose proper structures with compliant properties in order to optimize the static and dynamic performance.

Supporting structure plays an important role in gas foil journal bearing. Song and Kim¹¹ chose spring as the elastic support component with nonlinear stiffness, but the stiffness of the spring is too small to provide large load capacity. Hou et al.¹² experimentally studied a 25 mm rotor at the speed of 147,000 r/min using visco-elastic rubber as supporting

structure which cannot be applied to extreme environment. Later, Hou et al.¹³ performed a numerical study on single layer protuberant gas foil journal bearing and found out that the elastic support configuration benefits load capacity. Lee et al.¹⁴ placed visco-elastic material under the top foil and the new structure suppresses subsynchronous vibration of the rotor effectively. Andres and Chirathadam^{15,16} used simple and cost-effective bronze metal mesh as supporting structure to enhance the damping. Rubio and Andres¹⁷ tested the bump foil bearing stiffness using three shafts of different diameters; he found the

¹School of Energy and Power Engineering, Xi'an Jiaotong University, Xi'an, PR China

²Institute of Mechanical Manufacturing Technology, China Academy of Engineering Physics, Mianyang, PR China

³State Key Laboratory of Multiphase Flow in Power Engineering, Xi'an Jiaotong University, Xi'an, PR China

Corresponding author:

Yu Hou, School of Energy and Power Engineering, Xi'an Jiaotong University, 28 West Xianning Road, Xi'an 710049, PR China.
Email: yuhou@mail.xjtu.edu.cn

nonlinear deflection behavior of foil bearing as well as the hysteresis due to the friction between foil surfaces in the loading and unloading tests. The multi-layer configuration suppresses subsynchronous vibrations effectively. Kim and Andres¹⁸ analyzed multi-staged elastic bump foil bearing which could provide higher direct stiffness and damping.

In practical operation, gas film clearance and stiffness are changing with the rotor speed in the rotor speed-up and speed-down processes. The elastic support structure is required to adapt the clearance and stiffness to prevent the instability caused by changing rotation speed.⁹ It is necessary to investigate the effects of radial clearance and supporting structural stiffness on these transient processes.

In this study, the effect of radial clearance on the turboexpander performance is experimentally investigated. Protuberant foils with thickness of 0.05 mm and 0.07 mm are used as supporting structures. The effect of radial clearance on the rotor is compared

based on the relation between rotor speed and supply pressure in the speed-up and speed-down processes. The speed-up waterfalls and the rotor loci are compared to reveal the rotordynamic vibration characteristic under different radial clearances.

Experimental work

Multi-decked protuberant foil bearing

The schematic diagram of the multi-decked protuberant foil bearing is shown in Figure 1. The supporting structure is composed of three layers: top flat foil, upper protuberant foil (PF) and bottom PF. The ends of the three foils are aligned and pinned in a fixing hole while the other ends are free in the bearing housing.

The projections on the protuberant foil have spherical crown shape, and the distribution on the foil is shown in Figure 2(a). The arrangements of the two protuberant foils and the multi-decked configuration are shown in Figure 2(b) and (c), respectively. The protuberant structure array on the foil can be stamped from a flat beryllium bronze foil.

Test system and procedure

The photo of test rig used to examine the bearing performance in high-speed turboexpander is illustrated in Figure 3. The system consists of an air compressor, an air pressure buffer and a turboexpander. The pressurized air is supplied by the 75 kW ATLAS screw air compressor with supply pressure up to 1.3 MPa. The inlet gas is filtered to get rid of impurities. The inlet pressure of the expander is controlled through a regulating valve. The pressures at expander

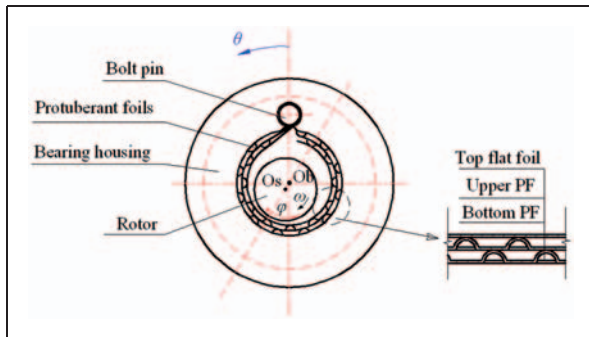


Figure 1. Schematic diagram of multi-decked protuberant gas foil bearing.

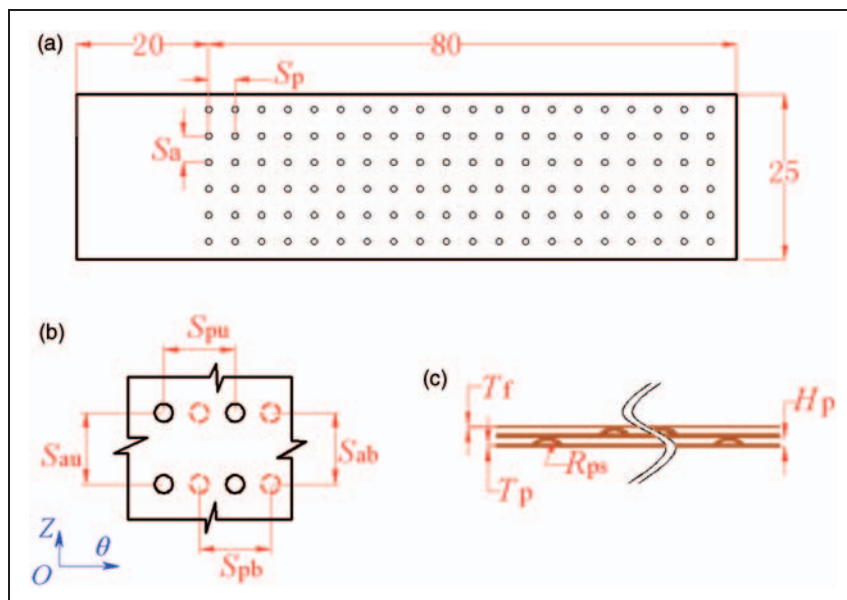


Figure 2. Protuberant foils features: (a) protuberant crown distribution; (b) arrangement of protuberant foils; (c) multi-decked foils.

inlet and hydrostatic bearing supply gas are monitored by pressure transducers.

The configuration of the tested turboexpander is shown in Figure 4. The rotor-bearing system is composed of expansion wheel, brake wheel, rotor, thrust bearings, and two foil journal bearings. The rotor is driven by high pressure gas at expansion wheel. Brake wheel is used to dissipate some of the mechanical work and balance part of the thrust force from expansion wheel. Two orthogonally positioned eddy current displacement sensors (with linearity $<\pm 2\%$ and static resolution of $0.1\ \mu\text{m}$) at middle section of the rotor are used to monitor the rotor vibration and rotational speed. The single row static thrust bearing is used to balance the thrust force with clearance around $30\ \mu\text{m}$.

The photo images of gas foil journal bearing pairs being tested are shown in Figure 5. The foils are

pinned into the bolt pin hole of the journal bearing housing. The upper foil of the bearing is made of beryllium bronze (QBe2) and coated with MoS_2 to reduce dry friction in start up and shut down processes. There is no wear resistant coat on the rotor. For convenience of comparison, the nominal radial clearance is changed using bearing housings of different inner diameters, while the same rotor is used.

The main parameters of the turboexpander and protuberant foil are listed in Table 1.

The tests procedure is listed below:

1. Set the supply pressure of static thrust bearing at $0.55\ \text{MPa}$ at the start-up process.
2. Turn up the regulation valve at the entrance of the turboexpander until the rotor lifts up from the

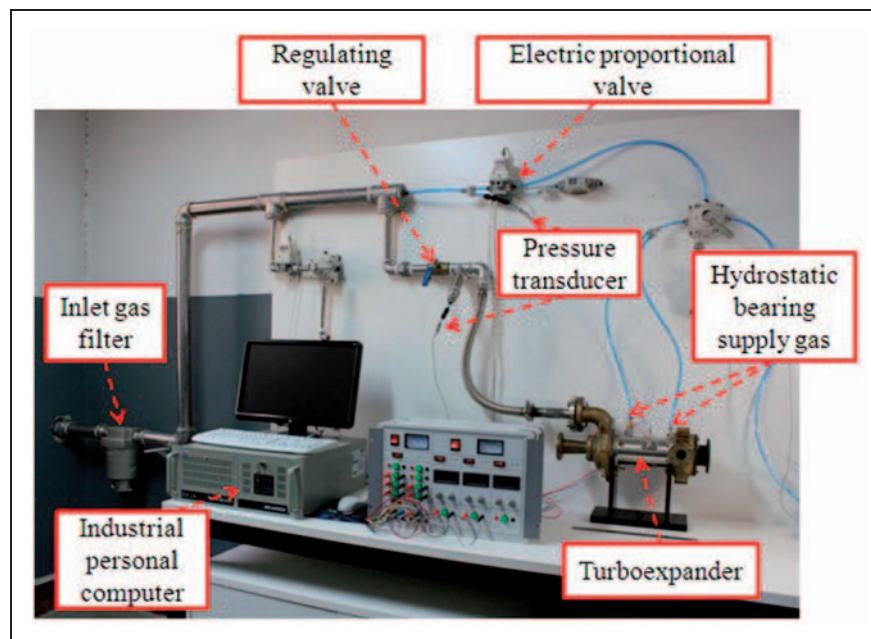


Figure 3. Experimental test rig.

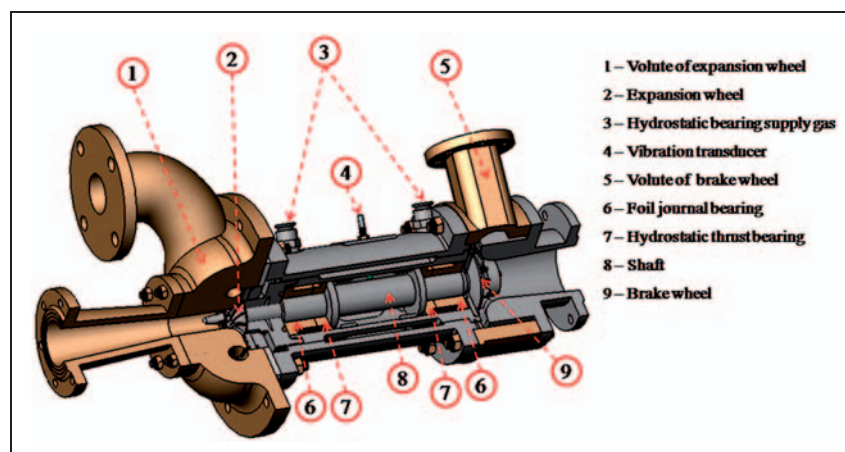


Figure 4. Configuration of tested turboexpander.

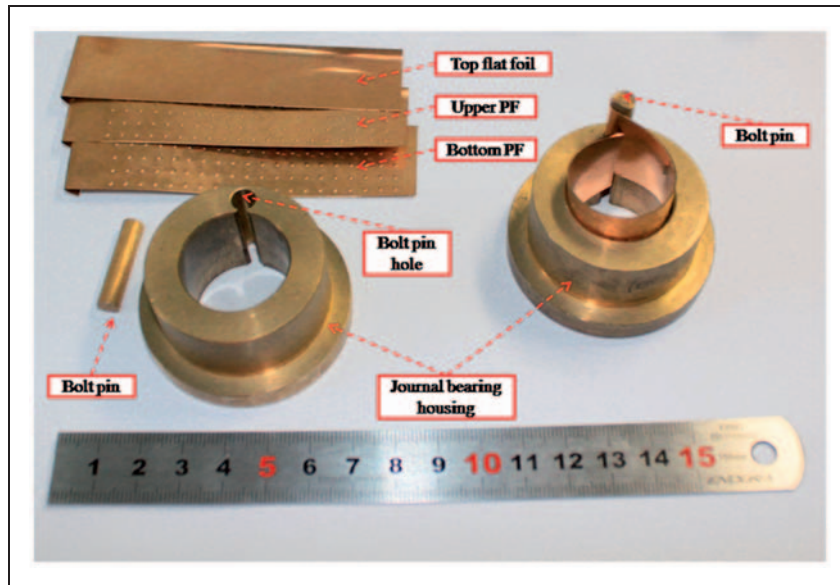


Figure 5. Tested journal gas foil journal bearing.

Table 1. Main parameters of the high-speed turboexpander.

Parameter	Magnitude	Parameter	Magnitude
D_1 (mm)	60	D_2 /mm	36.5
D_s (mm)	25	D_{in} /mm	28
D_{out} (mm)	44	L_r /mm	250.5
T_f (mm)	0.07	m_r /g	830
$S_{pu}, S_{pb}, S_{au}, S_{ab}$ (mm)	4	R_{ps} /mm	0.65

bearing, and gradually increase the supply pressure up to 1.15 MPa after the rotor lifting up. The relation between rotor speed and supply air pressure are sampled during start-up process.

3. Gradually turn off the regulating valve at the inlet of turboexpander until the rotor touches the bearing. The relation between rotor speed and supply air pressure is sampled during shutdown process.
4. Repeat the test for each bearing with bearing housing of different inner diameter.

Test results and discussion

Generally, the nominal clearance of compliant surface foil bearing is the overall magnitude of clearance. In reality, the actual clearance varies around the journal as a function of θ and along axial direction which is difficult to measure. The spheres on the protuberant foil are assumed to be stiff without deformation during the entire test. The nominal radial clearance of the multi-decked structure foil bearing is determined by

$$c = (D_h - D_s - 4H_p - 2T_f)/2 \quad (1)$$

Table 2. Nominal clearance in the tests.

No.	T_p (mm)	H_p (mm)	D_h (mm)	c (μm)
0	0.05	0.2	25.86	-20
1			25.9	0
2			25.94	20
3			25.98	40
4			26.02	60
5			26.06	80
6	0.07	0.22	26.02	0
7			26.06	20
8			26.1	40
9			26.14	60
10			26.18	80
11			26.22	100

where D_h is the inner diameter of bearing housing, D_s is the diameter of shaft, H_p is the height of protuberant foil, and T_f is the thickness of top foil, respectively.

Bearings with nominal clearances as shown in Table 2 are tested. Two protuberant foils with different foil thickness 0.05 mm and 0.07 mm are used in the bearings to investigate the effect of supporting stiffness on the bearing performance. The top flat foil can be obtained by tailoring bronze foil with neither wear-resistant material nor any heat treatment. The upper protuberant foil can be stamped from the flat foil by mold directly.

The 12 sets of experiment are conducted smoothly with good repeatability individually. Operating time for each pair of bearing lasts around 1.5 h.

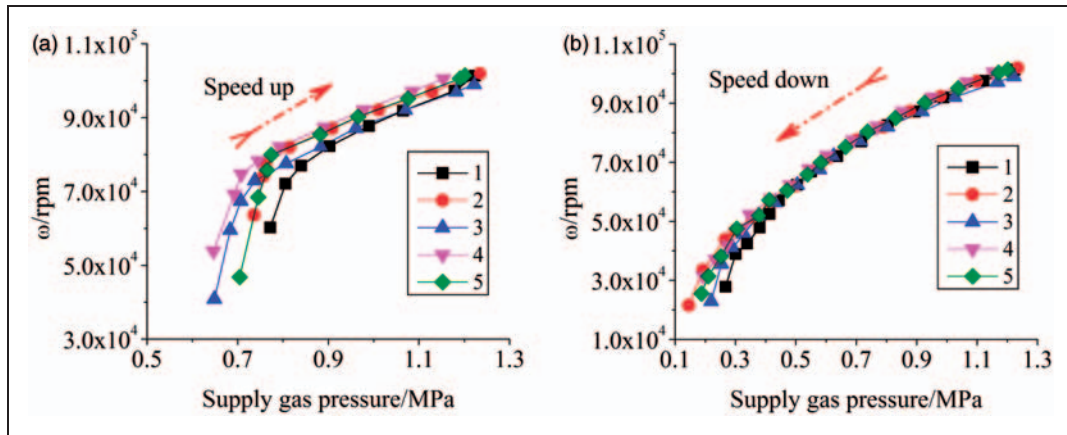


Figure 6. Rotor speed with supply gas pressures using 0.05 mm thickness protuberant foil.

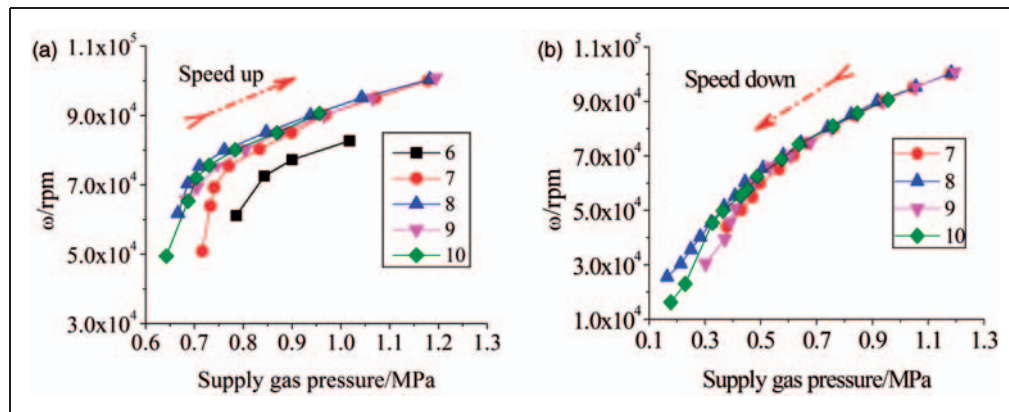


Figure 7. Rotor speed with supply gas pressures using 0.07 mm thickness protuberant foil.

Rotor speed to supply pressure

For bearings labeled with No. 0 to 5, the top flat foils are supported by protuberant foils of a 0.05 mm thickness. The relationship between rotor speed and supply air pressure in the speed up and speed down processes for bearings No. 1 to 5 are shown in Figure 6(a) and (b), respectively. For bearings No. 1 to 5, the measured minimal rotational speed is around 40,000 r/min to 60,000 r/min during the speed-up process. However, this minimal rotational speed is not necessarily the lift up speed, which is difficult to measure due to the fast transition and limited time response of data acquisition system. The speed-up process can be described in two stages: (1) the rotor speeded up quickly at the beginning as the supply air pressure increases; (2) after a certain pressure (0.7–0.9 MPa) the rotational speed increases with a smaller slope as the pressure is further increased. This two-stage speed-up process is determined by the gas expansion characteristics of turboexpander. Comparison of effects of clearance on rotor speed-up can be made at the same supply pressure during the speed-up process as shown in Figure 6(a). The rotation speed is smallest

for bearings with a $0 \mu\text{m}$ nominal clearance at any supply air pressure during the speed-up process. With the increase of clearance before $60 \mu\text{m}$, the rotational speed gets higher. The highest speed is obtained for bearing with a nominal clearance of $60 \mu\text{m}$. When the clearance further increases beyond $60 \mu\text{m}$, the rotor speed becomes smaller. The lower rotational speed for bearing with larger clearance can be attributed to the over relaxation of the bearing on the rotor which leads to the larger gas film thickness. In the speed down process, the trends of rotor speed-up with supply pressures are similar but of smaller variance for different nominal clearances. Compared to the two-stage process during speed-up, the rotational speed decreased gradually in the speed-down process.

In startup process, the coulomb friction between the foils impedes the relative movement of foils which leads to the increase the friction torque on the rotor as the rotational speed increases. However, in the speed-down process, the coulomb friction and the gas film friction are in opposite directions. Besides, the rotor lift up speed is higher than the landing speed in the experiment.

Table 3. Speed-up waterfall of the turboexpander with different elastic stiffness.

c (μm)	$T_p = 0.05$ mm	c (μm)	$T_p = 0.07$ mm
-20	(thermal runaway)	0	(thermal runaway)

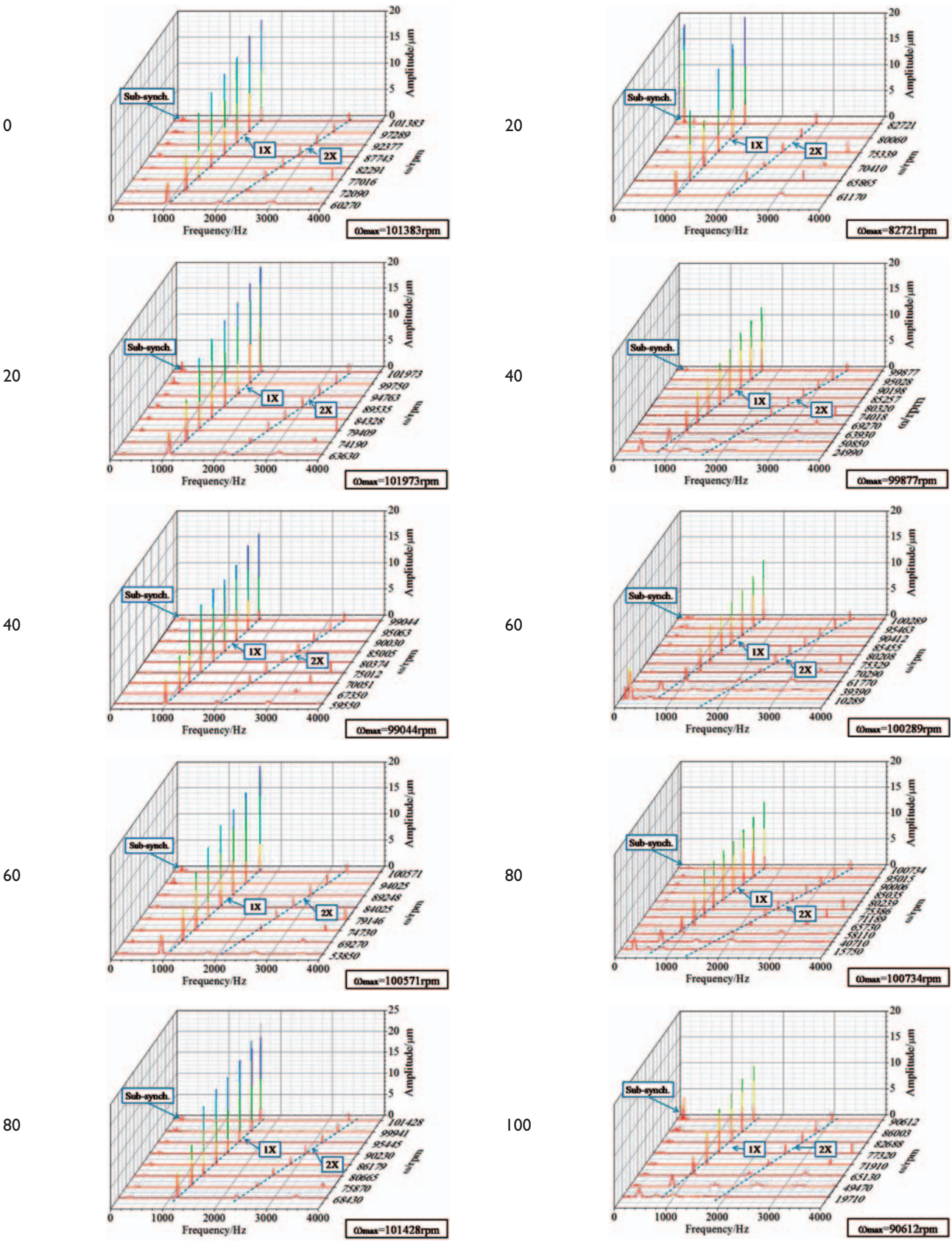
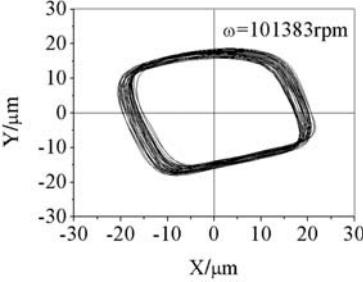
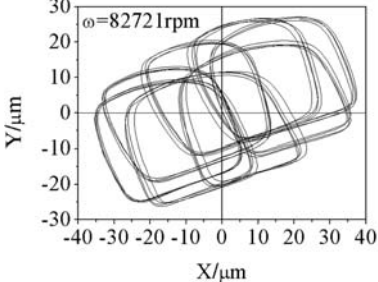
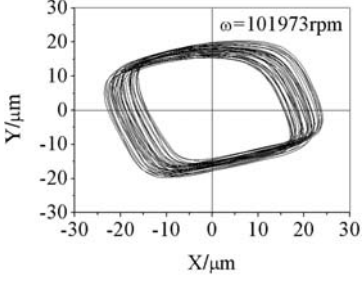
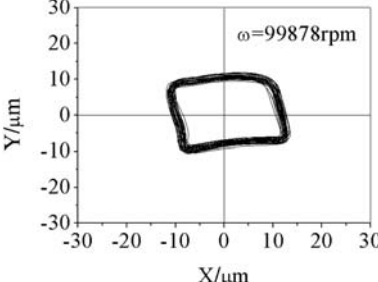
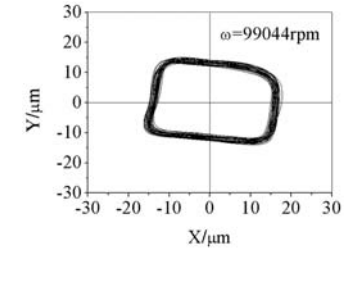
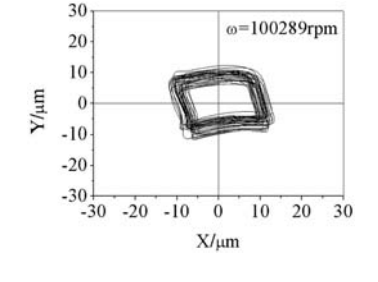
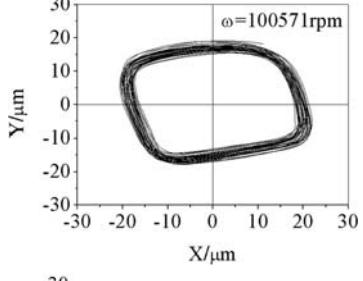
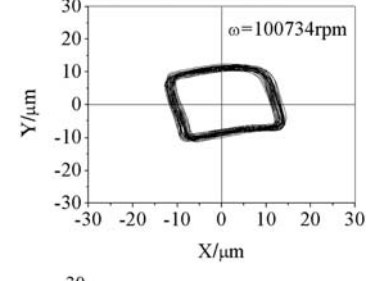
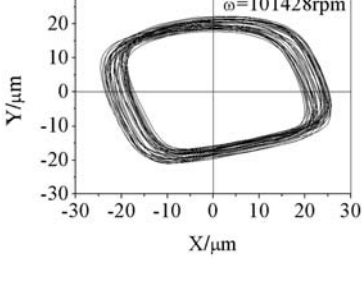
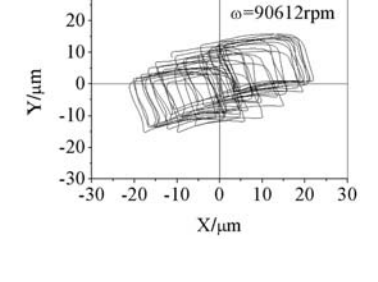


Table 4. Rotor locus at maximum speed.

c (μm)	$T_p = 0.05$ mm	$T_p = 0.07$ mm
-20	(thermal runaway)	(thermal runaway)
0		
20		
40		
60		
80		

For No. 6–11 bearings, the top flat foils are supported by 0.07 mm thickness protuberant foils. The relationship between rotor speed and supply gas pressure in the speed-up and speed-down processes are shown in Figure 7(a) and (b), respectively. The minimum rotor speed in the start-up process is around 50,000 r/min to 60,000 r/min.

Once the hydrodynamic pressure is built up in the gap between the rotor and top foil, the compliant deformation on top foil is produced to balance the hydrodynamic pressure. For the 0 μm clearance, the rotor speed is the smallest and the difference is more evident than that using 0.05 mm. With the increase of bearing clearance, the rotor speed gets higher and

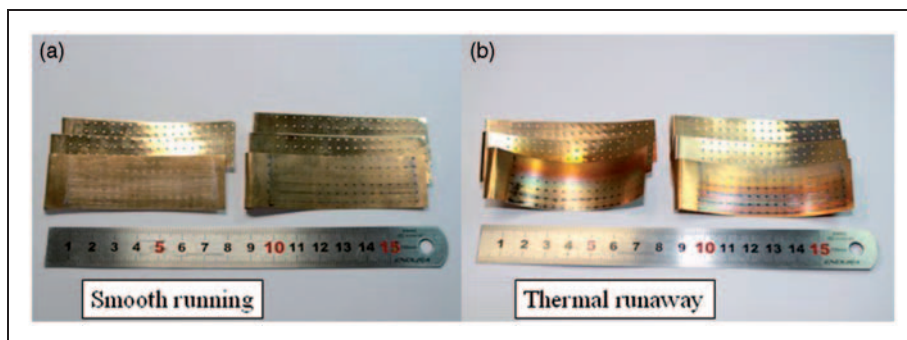


Figure 8. Foil journal bearing after use: (a) smooth running; (b) thermal runaway.

operates stably. When the clearance is around $40\ \mu\text{m}$, the rotor speed is the highest. Further increase of bearing clearance could result in lower rotor speed.

For the bearing, thicker protuberant supporting foils provide higher supporting stiffness and smaller elastic deformation. The relative motion between the foils is smaller with less coulomb friction.

Vibration character

The speed-up frequency content of rotor-bearing system with different nominal radial clearances and protuberant foil thicknesses are compared in the waterfalls in Table 3. For the $0.05\ \text{mm}$ protuberant foils, the bearing suffers from thermal failure with $-20\ \mu\text{m}$ clearance. With larger clearance from 0 to $80\ \mu\text{m}$, the bearing can provide moderate support for the turboexpander. The subsynchronous vibrations can be suppressed in the speed-up and speed-down processes as well as in high speed range. For the $0.07\ \text{mm}$ protuberant foils, which have stiffer support, the bearing suffers from thermal runaway under $0\ \mu\text{m}$ clearance at the rotational speed around $82,000\ \text{r/min}$ with high subsynchronous vibration.

In order to prevent the rotor from damage, the valve is shut down promptly due to unstable performance. When the radial clearance gets higher, the rotor runs smoothly with suppressed subsynchronous vibration. However, when the radial clearance is $100\ \mu\text{m}$, the rotor subsynchronous vibration amplitude exceeds that of the basic frequency (1X). Then, the inlet valve of the expander is turned down gradually. Andres et al.¹⁹ reported subsynchronous whirl frequency at around 50% shaft speed in bump foil bearings due to nonlinear stiffness characteristics. In this experiment, the subsynchronous vibrations are suppressed due to the multi-decked configuration which can be attributed to the damping effects of the multi-decked structure.

Rotor locus

The regularity and the orbit size of rotor with speed reflect the stability of the rotor supported by the bearing. The loci of the rotor supported by the bearings

with $0.05\ \text{mm}$ and $0.07\ \text{mm}$ protuberant foil under different radial clearances are shown in Table 4. The rotor loci are featured with the diamond shape due to the distinctive protuberant support structure. From 0 to $80\ \mu\text{m}$ clearance, the rotor loci of the bearings with $0.05\ \text{mm}$ protuberant foil support are regular and clear. The corresponding maximal speeds are around $100,000\ \text{r/min}$. For the bearing with $0.07\ \text{mm}$ protuberant foils, there are thermal failure problem around $0\ \mu\text{m}$ clearance and subsynchronous vibration with $80\ \mu\text{m}$ clearance. Overall, the rotor vibration magnitude using $0.07\ \text{mm}$ protuberant foil is smaller than that using $0.05\ \text{mm}$ protuberant foil which can be attributed to the stiffer support.

The protuberant foils after test are shown in Figure 8. The left bearing foils are the pair that perform well in the speed-up and speed-down test. The rubbed spots on the top foil correspond to the protuberant spheres of the supporting foil in Figure 8(a). The $0.05\ \text{mm}$ thickness protuberant foil of the thermal failed foil bearing with $-20\ \mu\text{m}$ clearance is shown in Figure 8(b). The top foil is heated from the original yellow bronze color into black. There is heat generated from the large velocity gradient in the gas film. Under normal circumstances, the heat can be dissipated through fluid convection or heat conduction in bearing structure. If the heat cannot be carried away promptly, the heat will accumulate in the bearing. The bearing suffers from thermal runaway for No. 0 bearing in that the heat generated by friction in the bearing could not be dissipated promptly.

Conclusion

The performance of multi-decked protuberant gas foil bearing in a high-speed turboexpander is investigated experimentally. The effects of radial clearance and elastic support stiffness on the rotor-bearing system in turboexpander are evaluated experimentally. For the turboexpander, the rotor speed of expander is lower with stiffer support and smaller radial clearance under the same supply pressure at expansion wheel. The subsynchronous vibrations are suppressed and the rotor runs smoothly. As for the nominal radial clearance tests, there is thermal runaway with

undersized clearance and subsynchronous vibration with oversized clearance. The eligible radial clearance range is narrower as the elastic support stiffness increases.

Funding

This project was supported by the National Basic Research Program of China (Grant No. 2011CB706505), Fundamental Research Funds for the Central Universities and NSAF (Grant No. 11176023), and partially supported by the Open Research Project of Key Laboratory of Cryogenics, TIPC, CAS (Grant No. CRYO201226).

Conflict of interest

None declared.

References

- Blok H and Van Rossum JJ. The foil bearing – A new departure in hydrodynamic lubrication. *Lubr Eng* 1953; 9(6): 316–320.
- Heshmat H and Hermel P. Compliant foil bearings technology and their application to high speed turbomachinery. *Thin Films Tribol* 1993; 25: 559–575.
- Agrawal GL. Foil air/gas bearing technology – an overview. ASME paper no. 97-GT-347, 1997.
- Dellacorte C, Lukaszewicz V, Valco MJ, et al. Performance and durability of high temperature foil air bearings for oil-free turbomachinery. *STLE Tribol Trans* 2000; 43(4): 774–780.
- Walton JF and Heshmat H. Application of foil bearings to turbomachinery including vertical operation. *ASME J Eng Gas Turbines Power* 2002; 124(4): 1032–1041.
- Howard SA, Dellacorte C, Valco MJ, et al. Steady-state stiffness of foil air journal bearings at elevated temperatures. *ASLE Tribol Trans* 2001; 44(3): 489–493.
- Howard S, Dellacorte C, Mark J, et al. Dynamic stiffness and damping characteristics of a high-temperature air foil journal bearing. *ASLE Tribol Trans* 2001; 44(4): 657–663.
- Hou Y, Zhu ZH and Chen CZ. Comparative test on two kinds of new compliant foil bearing for small cryogenic turbo-expander. *Cryogenics* 2004; 44(1): 69–72.
- Radil K, Howard S and Dykas B. The role of radial clearance on the performance of foil air bearings. *ASLE Tribol Trans* 2002; 45(4): 485–490.
- Heshmat H, Walowit JA and Pinkus O. Analysis of gas-lubricated foil journal bearings. *J Lubr Technol* 1983; 105(3): 647–655.
- Song J and Kim D. Foil gas bearing with compression springs: Analyses and experiments. *ASME J Tribol* 2007; 129(3): 628–639.
- Hou Y, Xiong LY and Chen CZ. Experimental study of a new compliant foil air bearing with elastic support. *STLE Tribol Trans* 2004; 47(2): 308–311.
- Hou Y, Chen ST, Chen RG, et al. Numerical study on foil journal bearings with protuberant foil structure. *Tribol Int* 2011; 44(9): 1061–1070.
- Lee YB, Kim TH, Kim CH, et al. Suppression of subsynchronous vibrations due to aerodynamic response to surge in a two-stage centrifugal compressor with air foil bearings. *STLE Tribol Trans* 2003; 46(3): 428–434.
- Andres LS and Chirathadam TA. Measurements of drag torque, lift-off journal speed, and temperature in a metal mesh foil bearing. *J Eng Gas Turbines Power* 2010; 132(11): 112503.
- Andres LS and Chirathadam TA. A metal mesh foil bearing and a bump-type foil bearing comparison of performance for two similar size gas bearings. *J Eng Gas Turbines Power* 2012; 134(10): 102501.
- Rubio D and Andres LS. Bump-type foil bearing structural stiffness: Experiments and predictions. *J Eng Gas Turbines Power* 2006; 128(3): 653–660.
- Kim TH and Andres LS. Analysis of advanced gas foil bearings with piecewise linear elastic supports. *Tribol Int* 2007; 40(8): 1239–1245.
- Andres LS, Rubio D and Kim TH. Rotordynamic performance of a rotor supported on bump type foil gas bearings: experiments and predictions. *J Eng Gas Turbines Power* 2007; 129(3): 850–857.

Appendix

Notation

c	nominal radial clearance (mm)
D_1	outside diameter of brake wheel (mm)
D_2	outside diameter of expansion wheel (mm)
D_h	bearing housing diameter (mm)
D_{in}	inside diameter of thrust bearing (mm)
D_{out}	outside diameter of thrust bearing (mm)
D_s	shaft diameter (mm)
H_p	height of protuberant foil (mm)
L_r	length of rotor (mm)
m_r	mass of rotor (g)
O_b	bearing center
O_s	shaft center
R_{ps}	radius of protuberant spherical crown (mm)
S_a	crown pitch in axial direction (mm)
S_{ab}	crown pitch in axial direction of bottom layer (mm)
S_{au}	crown pitch in axial direction of upper layer (mm)
S_p	crown pitch in peripheral direction (mm)
S_{pb}	crown pitch in peripheral direction of bottom layer (mm)
S_{pu}	crown pitch in peripheral direction of upper layer (mm)
T_f	top foil thickness (mm)
T_p	thickness of protuberant foil (mm)
X	vibration amplitude in X direction (μm)
Y	vibration amplitude in Y direction (μm)
Θ	circumferential coordinates (rad)
Φ	attitude angle (rad)
Ω	rotor speed (r/min)